Enhanced Atomic Transport at Liquid Metal/Al_2O_3 Interfaces

E. Saiz, R. M. Cannon, and A. P. Tomsia

Materials Sciences Division
Lawrence Berkeley National Laboratory
University of California,
Berkeley, CA 94720 USA

June 2000

Advanced Materials
in press

Work supported by the U.S. Department of Energy under Contract No. DE-AC03-76SF00098

.

The atomic theory of metal/oxide interfaces is in the early stages of formulation. Two of the main problems are the inherent complexity of many of the measurable interfacial properties (such us interfacial strength or friction) and the lack of systematic experimental data that could be contrasted with the theory. Because the continuum theory of capillary-driven mass transport is well established, measurement of the morphological evolution of interfaces can provide the basic data needed for understanding the atomic structure of metal/oxide boundaries. These "mesoscopic" experiments can also provide the intermediate step needed to link the atomic theory to technological processes such as composite sintering, refractory corrosion, metal-ceramic joining, thin-film stability, or supported metals catalysts. In this respect, the development of new characterization techniques, such as atomic force microscopy (AFM), provides an excellent opportunity for the accurate analysis of the topological evolution of surfaces and interfaces.[1]

One of the ways capillary mass transport manifests itself is by developing a grain boundary groove on the surface of a polycrystalline material wherever a boundary intersects an interface between a solid and another phase. The groove forms in order to achieve complete local equilibrium of the interfacial forces at the triple junction (groove root), and its growth results from transport of mass from the high curvature region near the root to the flatter parts of the interface. Mass transport can involve several mechanisms: interfacial diffusion, volume diffusion on either side of the interface, and interfacial reaction (solution-precipitation or evaporation-condensation if the fluid phase is liquid or gas, respectively). Depending on the physical characteristics of the system and groove size, one of these mechanisms will be rate controlling, resulting in characteristic groove shapes and growth kinetics.[2-5]

In the present work, AFM and scanning electron microscopy (SEM) were used to study the evolution of grain boundary grooves at the interface between liquid metals (Ni, Cu, Au, Al) and pure polycrystalline alumina. Our main objective was to determine the operative transport mechanisms at the interfaces and the corresponding diffusivities or solution-precipitation rates. The experiments have been performed at oxygen partial pressures for which the metal and the oxide coexist in equilibrium (no chemical reaction occurs at the interface). However, at some $p(O_2)$ adsorption can occur at all the interfaces involved (the metal and oxide surfaces and the metal/oxide

interface). It is expected that for all the studied metals with the exception of Al, a range of $p(O_2)$ exists where no adsorption takes place and all the interfaces are stoichiometric.[6]

The observed grain boundary grooves at all the solid/liquid interfaces were unexpectedly much wider than those at the solid/vapor interfaces (Figure 1). This result indicates for the first time that mass transport at the metal/ceramic interfaces is orders of magnitude faster than on the free surface. In every case, the shape of the groove, recorded using AFM line profiles perpendicular to the grooves, shows the presence of a hump on each side, corresponding to growth controlled by a diffusion mechanism.

Transport of Al_2O_3 involves diffusion of both Al and O ions or atoms. This diffusion could occur through the liquid metal, along the interfaces, or through the oxide itself. Based on known data for volume diffusion coefficients of alumina,[7] diffusion through the oxide is too slow to be considered. Although each species could move independently along either path, the dissolution and precipitation must involve stoichiometric Al_2O_3. Thus, the potential gradients for each species will be adjusted so that the sum of the departure or arrival rates from both paths are in stoichiometric proportion everywhere along the interface. Since the shape of an evolving groove is similar for either interfacial or volume controlled diffusion,[2-5] the fluxes from the two paths can be combined in a simple manner to give the rate of groove growth:

$$\frac{3w^3}{5^3}\frac{dw}{dt} = \frac{\left(2.7B_i^{Al} + wB_V^{Al}\right)\left(2.7B_i^{O} + wB_V^{O}\right)}{3\left(2.7B_i^{Al} + wB_V^{Al}\right) + 2\left(2.7B_i^{O} + wB_V^{O}\right)} \qquad [1]$$

where w is the groove width, measured as the distance between the two maximums (top of the humps) in the profile at both sides of the groove, and t is time. The interfacial and volume transport coefficients for each species (B_i, B_V) are:

$$B_i = \frac{\omega D_i \gamma_i \Omega}{kT} \qquad [2]$$

$$B_V = \frac{xD_V \gamma_i \Omega}{kT} \qquad [3]$$

Ω is the molecular volume, ω is the interfacial width, x is the molar solubility in the metal for the diffusing species, and D_i and D_v are the interfacial and volume diffusivities.

This model is analogous to the ambipolar coupling expected for creep or sintering, in which transport is limited by the slower species along its fastest path.[7-8] More rapid diffusion by either species over both paths would result in an additive relationship, in which the slow species would be controlling via interface transport at small grooves and volume transport would be limiting at large widths. For example, if oxygen transport were faster (as has been typically assumed for the free surface of Al_2O_3) Equation [1] reduces to:

$$\frac{3w^3}{5^3}\frac{dw}{dt} = \frac{\left(2.7B_i^{Al} + wB_V^{Al}\right)}{2} \qquad [4]$$

The qualitative trends would be similar if the diffusion species were complexes, e.g., AlO_x, assuming they have different stoichiometry than Al_2O_3.

Three kinds of fits have been attempted to discover which diffusion process is rate controlling:

$$w = 4.6\left(\frac{B_i t}{2}\right)^{1/4} + w_0 \text{ (interfacial diffusion control)} \qquad [5]$$

$$w = 5\left(\frac{B_V t}{2}\right)^{1/3} + w_0 \text{ (volume diffusion control)} \qquad [6]$$

$$w = 4.6\left(\frac{B_i t}{2}\right)^{1/4} + 5\left(\frac{B_V t}{2}\right)^{1/3} + w_0 \text{ (combined)} \qquad [7]$$

where w_0 is the initial width and B is the transport coefficient for the slower species. Note that although Equation (7) is only an approximate solution to Equation (4), extremely large errors result from fitting to the exact solution [4] because of its mathematical form. As an example, the evolution of the average groove widths, w, and the corresponding fittings for experiments in the Ni/Al_2O_3 system are presented in Figure 2. The results for all the systems are summarized in Table 1; the calculations assumed that $\Omega/2$, the volume per Al ion, is $2.12 \cdot 10^{-29}$ m^3, with γ_{sl} values taken from literature.[6, 9-10] The transport mechanism can be deduced by taking into account the physical implications of the calculated diffusivities and w_0 values as well as the comparison between the combined and single-mechanism fittings.

A range of oxygen activities exists for which the surface diffusivities measured for the free alumina surfaces did not depend on the presence of a metal drop on the substrate and were similar to the reported diffusivities for pure Al_2O_3 (Table 1). This agrees with the hypothesis that there is a range of $p(O_2)$ where no adsorption occurs and all the interfaces are stoichiometric. The slight

decrease of alumina surface diffusivites in the presence of Ni at oxygen partial pressures close to the equilibrium value for the reaction $Al_2O_3+Ni+(1/2)O_2 \rightarrow NiAl_2O_4$ (~1 Pa at 1500°C) could result from the adsorption of NiO_x species.[6]

For the Ni/Al_2O_3 interface, fittings to an interfacial-diffusion controlled process, as reflected by Equation (5), resulted very often in negative initial groove thickness (w_0). On the other hand, the volume diffusivities calculated from the combined and $t^{1/3}$ fittings are very similar, leading to the conclusion that, for the groove widths measured in this work, the rate-controlling mechanism is volume diffusion. The result of the $t^{1/4}$ fitting represents an upper limit for the contribution of interfacial diffusion, with the value calculated from the combined fitting being closer to the real one. The value of ωD_i from Equation [7] may be representative of interfacial diffusion and is in the range of values measured for the surface diffusion of alumina. If volume diffusion is the controlling mechanism, it has to be diffusion through the liquid. The Al self-diffusion coefficients in Al_2O_3 are more than three orders of magnitude smaller than those required (Table 1) and those for O are even smaller.[7] It is recognized that dissolved NiO and FeO are reported to enhance creep of Al_2O_3 under conditions considered to be controlled by lattice diffusion.[7,1] At the $p(O_2)$ values used here, however, the solubility is deemed to be too low to sufficiently influence the Al_2O_3 defect concentrations.

In the Au/Al_2O_3 system, the $t^{1/4}$ fitting for the air-annealed samples yields interfacial diffusivities like those measured on the surface of impure Al_2O_3. At a similar temperature and $p(O_2) = 10^{-10}$ Pa, the upper-bound interfacial diffusivity calculated for the Cu interface using Equation [5] is two orders of magnitude higher. Since a physical mechanism that could explain such a big difference in interfacial diffusivities at similar temperatures has not been formulated, the results suggest that grooving at the Cu interface is controlled by volume diffusion.

When the interfacial transport rates are controlled by volume diffusion, the diffusion of the species (Al, O, or some complexes of them) with the lower xD_V product will dictate grooving kinetics. Since, in the presence of Al_2O_3, aluminum and oxygen solubilities are related, $a_{Al}^2 a_O^3 = K(T)$, the grooving kinetics are expected to vary continuously with oxygen partial pressure. The observed dependence of xD_v on $p(O_2)$ observed in the Ni/Al_2O_3 systems suggests that, as expected,

diffusion of Al would be limiting at higher $p(O_2)$. However, at very low $p(O_2)$ diffusion, O could be limiting. Assuming a volume diffusion coefficient of $D_V \approx 10^{-9}$ $m^2 \cdot s^{-1}$ (a typical value for liquid metals)[11], the estimated molar solubility of the slow species in Ni is $\sim 10^{-4} - 10^{-6}$ depending on the oxygen partial pressure. This seems plausible compared to measurements of Al or O solubility in liquid Fe[12] and solid Ni[13] in equilibrium with Al_2O_3. The results imply a solubility of $\sim 10^{-6}$ for Cu and several orders of magnitude lower for Au. (Obviously, further work is necessary to clarify these points.)

The interfacial diffusivities should not depend on the oxygen partial pressure when there is no adsorption, but with oxygen or aluminum adsorption, some variation could be expected. Because Al and O activities are related, reducing the activity of oxygen increases the activity of Al in the liquid. For many metal-aluminum systems, all the compositions in the binary system are molten at temperatures just above the melting point of the metal M, resulting in a fully miscible liquid metal phase. Then, the composition of the liquid in equilibrium with alumina is nearly pure Al at the low $p(O_2)$ phase boundary and increases rapidly in its M content with rising oxygen activity. It becomes nearly pure M after an orders-of-magnitude increase in $p(O_2)$.[6] Thus, study of the Al/Al_2O_3 interface should reveal trends expected at very low oxygen activity.

The shapes of the grain boundary grooves formed at 1373 K on the Al/Al_2O_3 interface correspond to diffusion-controlled growth, albeit perturbed by faceting. However, mass transport is several orders of magnitude faster than at or near the stoichiometric Au or Cu/Al_2O_3 interfaces at similar temperatures. Comparison of the $t^{1/3}$, $t^{1/4}$, and combined fittings (Table 1) suggests that the transport is primarily at the interface, but the data are not good enough to eliminate the possibility of volume diffusion from making a large or even dominant contribution to groove growth. The estimated solubility of O from very limited data, $\sim 8 \cdot 10^{-6}$, is consistent with transport along both paths and less than implied for transport exclusively through the liquid.[14] Most strikingly, the upper limit for the interfacial diffusivity ($t^{1/4}$ fitting) and the value from the combined equation are similar and far larger than ever reported for any alumina surfaces.[15] However, most of the values reported for alumina have been from experiments performed at oxygen pressures far larger than the one at which Al and Al_2O_3 coexist in equilibrium. At the low $p(O_2)$ limit of the metal/alumina coexistence

range, some variation could be expected as a result of adsorption and the formation of an Al-rich interface.[6] The relevant interface diffusivity in the Al/Al_2O_3 system would likely be that for O instead of Al.

In experiments to investigate the effect of low $p(O_2)$ on the surface diffusion of pure alumina, we made an important discovery. The calculated surface diffusivity (Table 1) is orders of magnitude greater than any observed before.[15] These experiments were carried out in gettered Ar, with an Al_2O_3 substrate in a closed alumina crucible close to an Al drop. It is expected that, under those conditions, the $p(O_2)$ inside the crucible would be close to the phase boundary value for the Al/Al_2O_3 system. Most of the boundary grooves that formed on the alumina have a shape expected for a diffusion-controlled process (although faceting altered the shape of some). Note that the previous reported data for the surface diffusivity of alumina has been taken at much higher $p(O_2)$. Although vapor transport may be suspected, the implied $t^{1/2}$ fit was unsatisfactory. These differences between the Al/Al_2O_3 system and the stoichiometric interfaces (Ni, Cu, Au) may be consistent with there being an excess of Al at both the surfaces and interfaces. This excess of Al would underline the often-neglected effect of oxygen activity on the oxide surface properties.

Another important and unexpected difference between the Al/Al_2O_3 and the stoichiometric interfaces is that the former appears to be much more anisotropic (Figure 3). The Al/Al_2O_3 interfaces are strongly faceted, and the hexagonal shape of some facets suggests that the alumina basal plane is a low energy surface when in contact with Al. In contrast, the interfaces with Ni appear to be very nearly isotropic, with smooth and rounded shapes and only a few visible facets, more isotropic than the free surface of alumina seen here and elsewhere.[16,17] The Al_2O_3 surfaces outside the Al drops seem to be less strongly faceted than those under Al, but somewhat more so than the stoichiometric surfaces of Al_2O_3. Such enhanced faceting is in part a result of more rapid transport, but the basal plane has clearly become relatively more stable for the interface and seemingly also for the surface.

The effect of oxygen activity on the interfacial anisotropy has not been systematically studied. Our results indicate a change in the Wulff plot for the sapphire-vapor surface versus those recently reported[18,19] for higher oxygen activities, which would be consistent with the idea that the surfaces

oriented parallel to alternating sheets of O and Al atoms in the crystal structure may be partially reduced more readily. The (0001) plane has been shown to become Al rich in UHV.[20-21] Evidently, the situation is analogous for the liquid Al/Al_2O_3 interface.

The results presented here provide fundamental data necessary for the modeling of those technological processes involving the interaction between liquid metals and oxides. These results also provide data needed for the development of an atomic theory of kinetic processes at metal/ceramic interfaces. Such a theory should provide a basis for understanding the relation between the diffusivities at the metal/ceramic interfaces and the oxide surface. It should account for the observed fast transport rates near the metal/oxide interface and the observed increase in transport rates at very low oxygen activities. It should also explain the observed transition from the isotropic stoichiometric interfaces to the anisotropic ones observed at very low oxygen activity, when adsorption is expected to occur.

Experimental

Small pieces of the selected metals were melted at different oxygen partial pressures on pure alumina substrates for different times. Experiments with Au in air were performed inside a closed sapphire crucible, embedded in Al_2O_3 powder. The polished alumina substrates had an average grain size of 20 μm. After firing, the metals were chemically etched, and SEM and AFM were used to analyze the area under the metals. The profiles of the boundary grooves at the solid/liquid and solid/vapor interfaces were measured using AFM line analysis in the constant-force mode. Between 80 and 100 boundaries were measured for each sample. To study the evolution of grooves with time, pieces of the metals were consecutively melted at the same place on the substrate, and the interface was analyzed after sequential heating and etching steps. This process was repeated two to six times. Al/Al_2O_3 experiments were also carried out in gettered Ar, placing an Al_2O_3 substrate in a closed alumina crucible, close to an Al drop.

Acknowledgments

This work was supported by the Director, Office of Energy Research, U.S. Department of Energy, under contract No. DE-AC03-76SF00098.

References

1. M. Ruehle, *Advanced Materials*, **9**, 1997, 195.
2. W. W. Mullins, *J. Appl. Phys.*, **28**, 1957, 333.
3. W. W. Mullins, *Trans. Met. Soc. AIME*, **218**, 1960, 354.
4. W. W. Mullins and P. G. Shewmon, *Acta Metall.*, **7**, 1959, 163.
5. W. M. Roberston, *J. Appl. Phys.*, **42**, 1971, 463.
6. E. Saiz, A. P. Tomsia, R. M. Cannon in *Ceramic Microstructures: Control at the Atomic Level*, A. P. Tomsia and A. M. Glaeser, Ed., Plenum Press, N. Y.,1998, 65.
7. R. M. Cannon and R. L. Coble, *Deformation of Ceramic Materials*, ed R. C. Bradt and R. E. Tressler, Plenum Press, N. Y., 1975, 61.
8. R. S. Gordon, *J. Am. Ceram. Soc.*, **56**, 1973, 147.
9. K. Nogi, K. Oishi, K. Ogino, *Mater. Trans., JIM*, **30**, 1989, 137.
10. J.-G. Li, *J. Amer. Ceram. Soc.*, 75, 1992, 3118.
11. C. J. Smithells, Ed., *Metals Reference Book*, (Butterworths, London & Boston, 1976) pp. 939.
12. G. R. Holcomb and G. R. St. Pierre, *Metall Trans B*, **23B**, 1992, 789.
13. K. P. Trumble and M. Rühle, *Acta Metall. Mater*., **39**, 1991, 1915.
14. H. A. Wriedt, *Bull. Alloy Ph. Diag.*, **6**, 1985, 548.
15. J. M.. Dynys, R. L. Coble, W. S. Coblenz, R. M. Cannon, *Sintering Processes*, ed. G. C. Kuczynski, Plenum Publishing Corporation, 1980, 391.
16. C. A. Handwerker, J. M. Dynys, R. M. Cannon, R. L. Coble, *J. Am. Ceram. Soc.*, **73**, 1990, 1365.
17. C. A. Handwerker, J. M. Dynys, R. M. Cannon, R. L. Coble, ibid., 1371.
18. J. –H. Choi, D. –Y. Kim, B. J. Hockey, S. M. Wiederhorn, C. A. Handwerker, J. E. Blendell, W. C. Carter, A.R . Roosen, *J. Am. Ceram. Soc.*, **80**, 1997, 62.
19. M. Kitayama, and A. M. Glaeser, *Key Eng. Mater*., **159-160**, 1998, 193.
20. T. M. French and G. A. Somorjai, *J. Phys. Chem*., **74**, 1970, 2489.
21. M. Gautier, G. Renaud, L. P. Van, B. Villette, M. Pollak, N. Thromat, F. Jollet, J. –P. Duraud, *J. Am. Ceram. Soc*., **77,** 1994, 323.

Figure Captions

Figure 1. SEM image of an alumina substrate after removing a Ni drop (melted for 1 hour at 1773 K). Grain boundary grooving is enhanced in the area under the liquid.

Figure 2. Time evolution of average groove widths at the surface of alumina and selected Al/Al_2O_3 and Ni/Al_2O_3 interfaces. Fittings to $t^{1/3}$ (volume diffusion) and $t^{1/4}$ (surface diffusion) laws are shown.

Figure 3. AFM images of alumina substrates after removing (a) Ni (melted 1 hour at 1773 K, $p(O2) = 10^{-10}$ Pa) and (b) Al (melted 15 minutes at 1773 K, $p(O2) = 10^{-17}$ Pa).

Table 1. Calculated surface and volume diffusivities at the M/Al2O3 interfaces as well as on the Al surface outside the metal drop (denoted Al_2O_3(M)). The * denotes those interfaces expected to be stoichiometric (with no adsorption).

System	$p(O_2)$ (Pa)	Temp (K)	Surface Diffusion		Volume Diffusion		Combined		
			$\omega \cdot D_i$ ($m^3 \cdot s$)	w_0 (nm)	$x \cdot D_v$ ($m^2 \cdot s$)	w_0 (nm)	$\omega \cdot D_i$ ($m^3 \cdot s$)	$x \cdot D_v$ ($m^2 \cdot s$)	w_0 (nm)
Al_2O_3*	10^{-10}	1873	$4.6 \cdot 10^{-21}$	0					
Al_2O_3 (Ni)*	10^{-10}	1773	$2.0 \cdot 10^{-22}$	0					
Al_2O_3 (Ni)	1	1773	$4.2 \cdot 10^{-23}$	0					
Al_2O_3 (Al)	10^{-17}	1773	$2.6 \cdot 10^{-18}$	2688					
Ni/Al_2O_3*	10^{-10}	1773	$4.4 \cdot 10^{-19}$	-795	$1.1 \cdot 10^{-13}$	525	$8.4 \cdot 10^{-22}$	$5.9 \cdot 10^{-14}$	220
Ni/Al_2O_3	1	1773	$3.0 \cdot 10^{-20}$	-39	$1.6 \cdot 10^{-14}$	25	$7.6 \cdot 10^{-23}$	$8.6 \cdot 10^{-15}$	0
Au/Al_2O_3*	$2 \cdot 10^{4}$	1373	$1.8 \cdot 10^{-24}$	195	$3.5 \cdot 10^{-18}$	385			
Cu/Al_2O_3*	10^{-10}	1423	$2.8 \cdot 10^{-22}$	0	$7.8 \cdot 10^{-16}$	0			
Al/Al_2O_3	10^{-26}	1373	$1.1 \cdot 10^{-19}$	-162	$5 \cdot 10^{-14}$	630	$4.1 \cdot 10^{-20}$	$6.6 \cdot 10^{-16}$	0

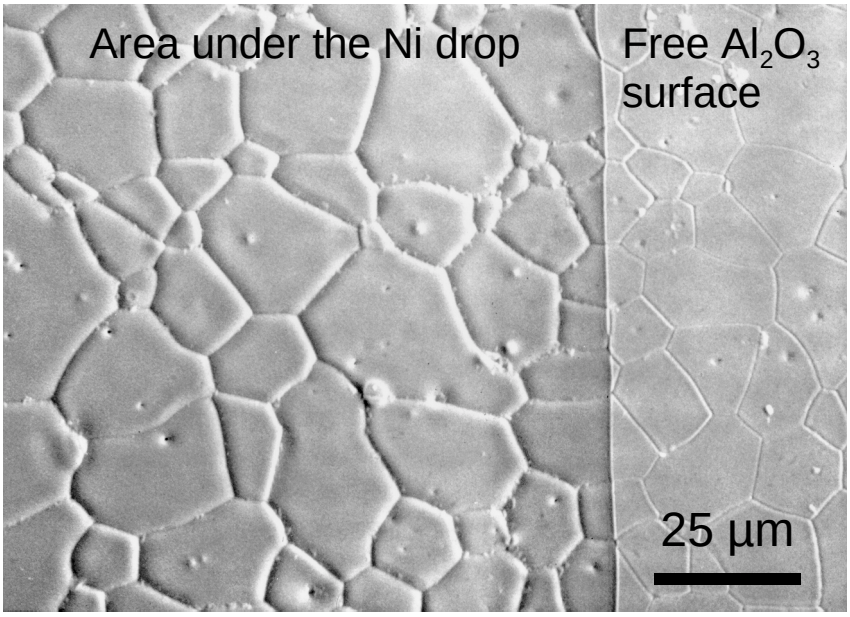

Figure 1

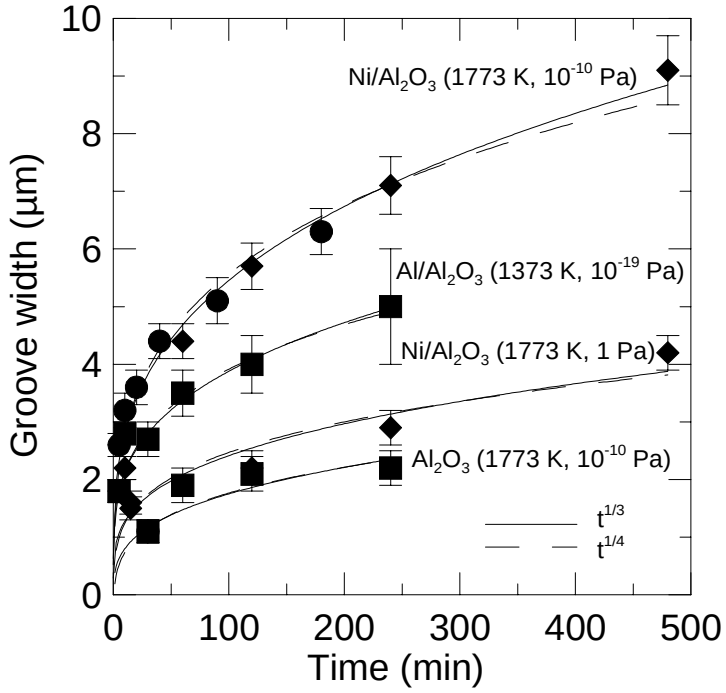

Figure 2

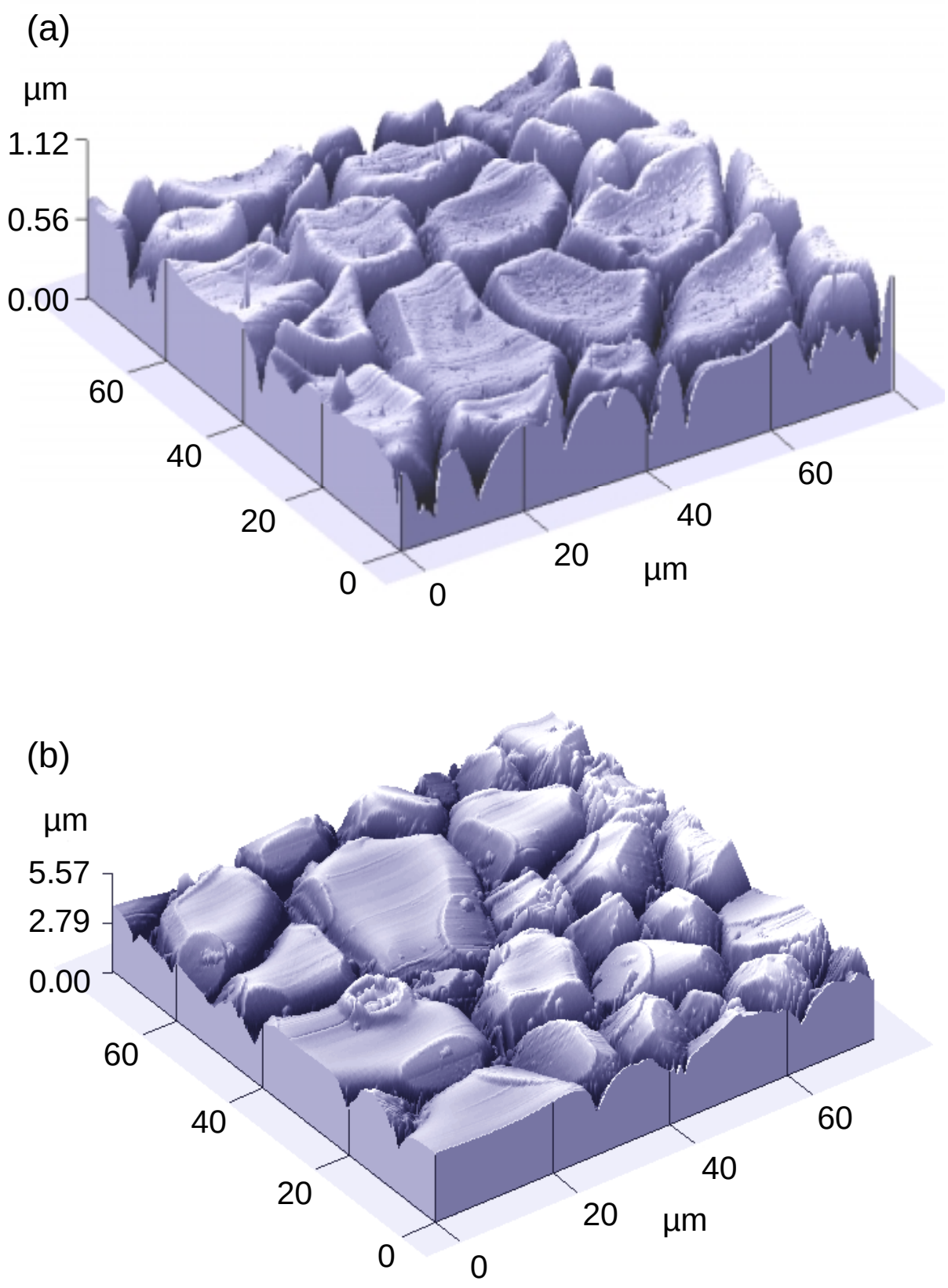
(a)
µm
1.12
0.56
0.00
60
40
20
0
0
20
40
60
µm
(b)
µm
5.57
2.79
0.00
60
40
20
0
0
20
40
60
µm

Figure 3